Available online at www.sciencedirect.com
ScienceDirect
Ceramics International 34 (2008) 1419–1423
CERAMICS INTERNATIONAL
www.elsevier.com/locate/ceramint

Sintering of binderless WC–Mo_2C hard materials by rapid sintering process

Hwan-Cheol Kim, Hyun-Kuk Park, In-Kyoon Jeong, In-Yong Ko, In-Jin Shon *

Department of Advanced Materials Engineering, Research Center of Advanced Materials Development, Chonbuk National University, Jeonju, Jeonbuk 560-756, Republic of Korea

Received 19 February 2007; received in revised form 5 March 2007; accepted 27 March 2007
Available online 6 May 2007

Abstract

High-frequency induction heated sintering (HFIHS) is a new rapid sintering method which was developed recently for the fabrication of ceramics and composites. This method combines a short time high-temperature exposure with pressure application. In this work, we reported results on the sintering of binderless WC–x wt.%Mo_2C ($0 \leq x \leq 6$) hard materials using ultra fine powders of WC and Mo_2C. A complete densification of the materials was achieved within 1 min. The relative densities of the composites were about 99% for an applied pressure of 60 MPa and an induced current for 90% output of total capacity. The Vickers hardness decreased and the fracture toughness increased with increasing the Mo_2C content.

Keywords: C. Mechanical properties; Rapid sintering; Binderless carbides; Hard materials; Microstructures

1. Introduction

Many of the transition metal carbides (e.g., WC, TaC, and TiC) are high melting-temperature compounds with high hardness, high thermal and electrical conductivities, and a relatively high chemical stability. They are primarily used as cutting tool and abrasive materials in single-phase and composite structures. In the latter case, their use as cemented carbides (particularly WC) involves the formation of a composite with a binder metal, such as Co or Ni. Tungsten carbide has a high melting point (a peritectic melting temperature of 2785 °C) and high hardness (16–22 GPa Vickers at 500 g load) [1,2]. In addition to its use as a cutting material, it has been considered for other uses such as a catalyst (substituting for noble metals) [3–5], as a catalyst electrode in fuel cells, and as a coating for aerospace components [6].

Cemented carbides are widely used for wear parts in various applications, i.e., face seals, tools for metal cutting and rock drilling. Binderless carbides have been developed as a complement to conventional cemented carbides for use in corrosive environments where the metal binder degrades [7]. Normally a binderless carbide has a lower abrasion resistance than metal-rich cemented carbides, but higher than that of common engineering ceramics. The main advantages of the materials over other ceramics in wear applications is its ability to withstand high pressures and speed in sliding contact without microfracturing [8].

When conventional sintering processes are used to sinter nano-sized powders, concomitant grain growth leads to the destruction of the nanostructure. This focuses attention on consolidation methods in which grain growth can be eliminated or significantly reduced. To accomplish this, rapid sintering methods have been widely used to sinter nano-sized powders. The most obvious advantage of rapid sintering is that fast heating and cooling rates, and the short dwell time lead to bypassing low-temperature, non-densifying mass transport (e.g., surface diffusion) [9,10]. However, conventional rapid heating can lead to temperature gradients and thus differential densification (non-uniform microstructures), low density, or specimen cracking. To overcome these difficulties, other rapid sintering techniques, such as the spark plasma sintering (SPS) method [11,12], have been developed.

High-frequency induction heated sintering (HFIHS) is a new rapid sintering method which was developed recently for the

* Corresponding author.
E-mail address: ijshon@chonbuk.ac.kr (I.-J. Shon).

0272-8842/$34.00
doi:10.1016/j.ceramint.2007.03.029

fabrication of ceramics and composites [13–16]. This method combines a short time, high-temperature exposure with pressure application. During the HFIHS, a large current will be induced in the sample and in the graphite die. As a result, the sample can be sintered uniformly and rapidly. In this work, we report results on the sintering of binderless WC–Mo_2C hard materials by a rapid sintering process, high-frequency induction heated sintering (HFIHS) methods which combine induced current with high-pressure application. The goal of this work is to produce dense, ultra-fine WC–x wt.%Mo_2C ($0 \leq x \leq 6$) cermets in very short sintering times (<1 min). And we investigated the effect of Mo_2C contents on the mechanical properties of WC–Mo_2C cermets.

2. Experimental procedure

The tungsten carbide powder used in this research was supplied by TaeguTec Ltd. (Taegu, Korea). The powder had a grain size of 0.4 μm measured by a Fisher sub-sieve sizer (FSSS) and was reported to be 99.5% pure. The Mo_2C powder obtained from Alfa Products (Ward Hill, MA, USA) was used. The powder had a grain size of 325 mesh measured by specific surface area (SSA) and was reported to be 99.5% pure. All powders were milled in a Universal Mill with a ball-to-powder weight ratio of 6:1. Milling was done in polyethylene bottles with diameter of 7.5 cm using tungsten carbide balls (size of 8 mm) and was performed at a horizontal rotation velocity of 250 rpm for 24 h. Ethanol was used by milling fluid.

The powders were placed in a graphite die (outside diameter, 45 mm; inside diameter, 20 mm; height, 40 mm) and then

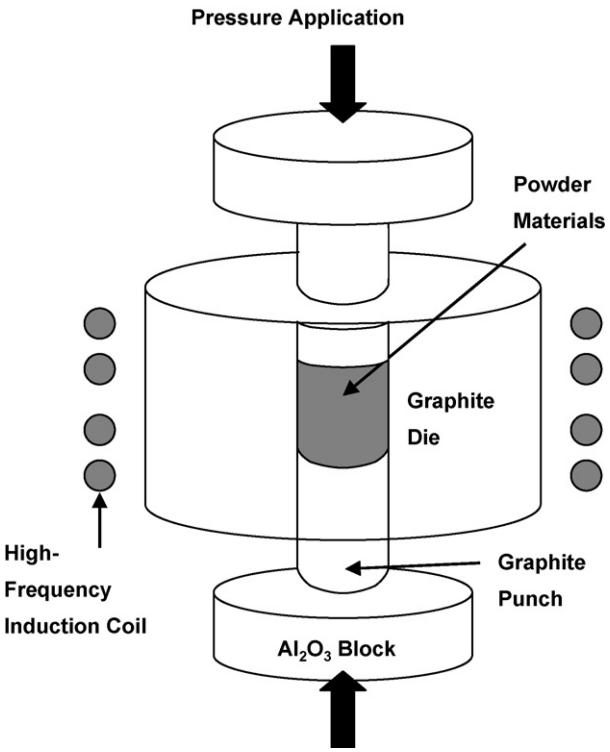

Fig. 1. Schematic diagram of apparatus for high-frequency induction heated sintering.

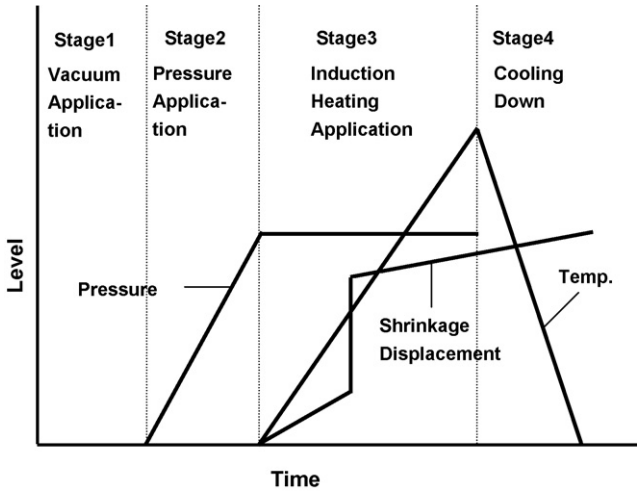

Fig. 2. Schematic representation of the temperature, pressure and shrinkage displacement profile during HFIHS.

introduced into the high-frequency induction heated sintering system made by Eltek Co. in Republic of Korea. Schematic diagrams of this method are shown in Fig. 1. The system was first evacuated and a uniaxial pressure of 60 MPa was applied. An induced current (frequency of about 50 kHz, 90% output of total power capacity, 15 kW) were then activated and maintained until the densification rate was negligible, as indicating by the observed shrinkage of the sample. Sample shrinkage is measured in real time by a linear gauge measuring the vertical displacement. Temperatures were measured by a pyrometer focused on the surface of the graphite die. Depending on heating rate, the electrical and thermal conductivities of the compact, and on its relative density, a difference in temperature between the surface and the center of the sample exists. At the end of the process, the induced current was turned off and the sample was allowed to cool to room temperature. The entire process of densification using the HFIHS technique consists of four major control stages. These are chamber evacuation, pressure application, power application, and cool down. The four major stages in the sintering are shown schematically in Fig. 2. The process was carried out under a vacuum of 40 mTorr.

The relative densities of the sintered samples were measured by the Archimedes method. Microstructural information was obtained from product samples, which had been polished and fractured at room temperature. Compositional and microstructural analyses of the products were made through X-ray diffraction (XRD) and scanning electron microscopy (SEM) with energy dispersive spectroscopy (EDS). Vickers hardness was measured by performing indentations at a load of 10 kg_f and a dwell time of 15 s. The carbide grain size, d_{WC} was obtained by the linear intercept method [17,18].

3. Results and discussion

The variations of shrinkage displacement and temperature with heating time during the sintering of WC and WC–6 wt.%Mo_2C hard materials using high frequency induction

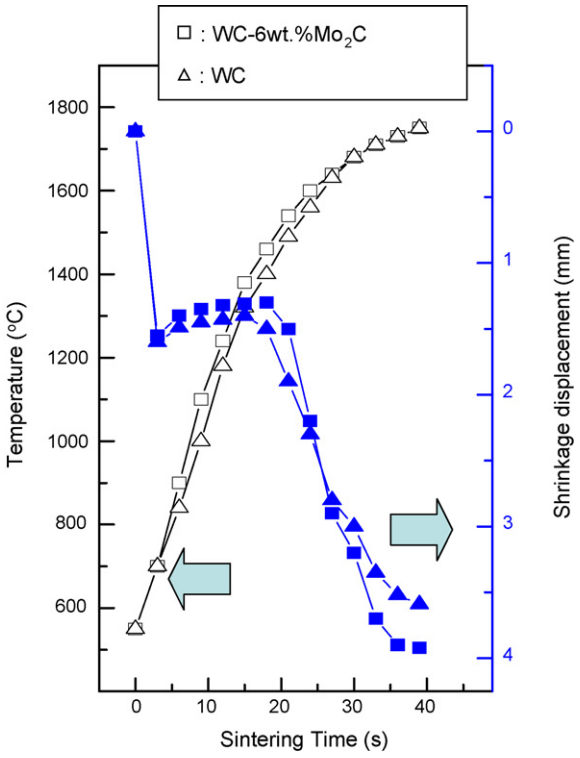

Fig. 3. Variations of temperature and shrinkage displacement with heating time during high-frequency induction heated sintering of WC–Mo_2C hard materials (under 60 MPa pressure, 90% output of total power capacity).

sintering with 90% output of total power capacity under a pressure of 60 MPa pressure are shown in Fig. 3. In both cases, initially the sample exhibits an increase in volume due to thermal expansion. As the electric current is applied, the shrinkage displacement decreased up to about 1500 °C, and then abruptly increased as the temperature is further increased from this value. When the temperature reaches about 1700 °C, the densification rate becomes nearly negligible, and as will be seen later, the samples have densified to 99% of theoretical

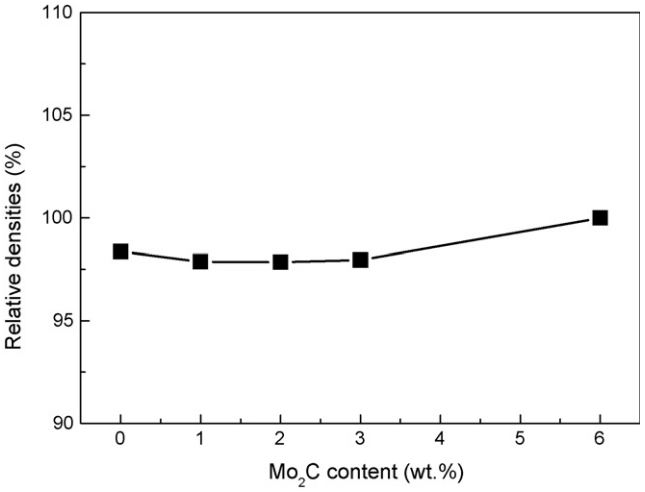

Fig. 4. Relative density of binderless WC–*x* wt.%Mo_2C hard materials produced by HFIHS.

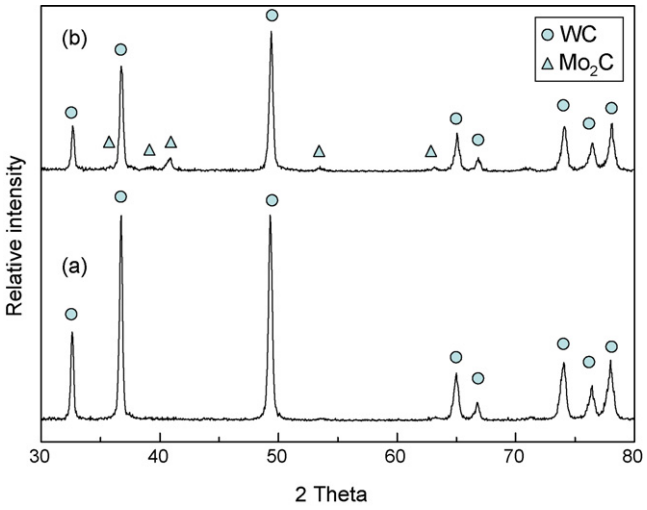

Fig. 5. XRD patterns of WC–Mo_2C hard materials sintered by HFIHS (a) WC and (b) WC–6 wt.%Mo_2C.

density in about 40 s. The observation of the onset of sintering was not affected by the contents of Mo_2C.

The dependence of relative density of the WC–Mo_2C hard materials on Mo_2C content for samples produced by the HFIHS method is shown in Fig. 4. The samples have densified to 98.5% of the theoretical density in about 40 s for all cases of WC–Mo_2C composites. With increasing the Mo_2C contents, the relative density of WC–Mo_2C composites increased slightly. The attainment of higher density and finer structure in a short time using induced current heating with pressure is not well understood. However, we would suggest that the HFIHS densification may be attributed to a combination of electrical discharge, resistance heating, and pressure application effects [19]. The role played by the current has been variously interpreted, the effect being explained in terms of fast heating rate due to Joule heating, the presence of plasma in pores separating powder particles, and the intrinsic contribution of the current to mass transport. So we would suggest that the HFIHS densification may be attributed to a combination of fast heating rates and intrinsic effects on mass transport.

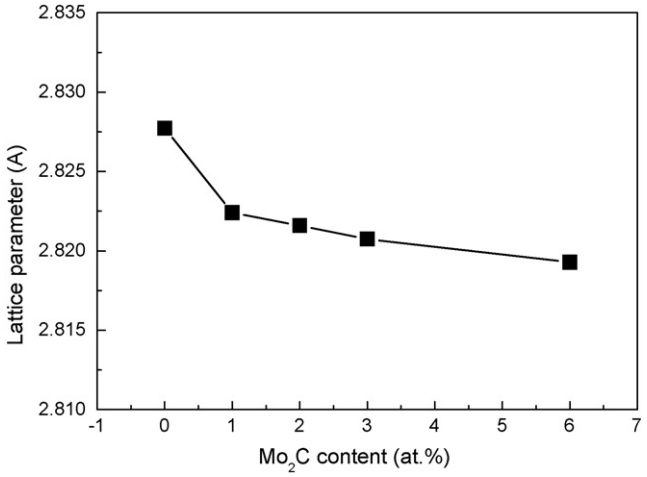

Fig. 6. Plot of WC phase lattice parameter a in the function of Mo_2C hard materials produced by HFIHS.

The nature of the products of sintering is revealed in Fig. 5, which shows the XRD patterns of WC and WC–6 wt.%Mo_2C hard materials after sintering by HFIHS in this work. In the case of pure WC, only peaks belonging to WC are seen, indicating that no compositional changes took place during the sintering. No peaks for the sub-carbide W_2C or any impurity phase are present. In the case of WC–Mo_2C cermets, only WC and Mo_2C peaks were observed. In XRD patterns of products, we could not find the peaks of solid solution because solid solution peaks was overlapped with that of Mo_2C. So we calculated the lattice parameter, a, of tungsten carbide using the XRD results. Fig. 6 shows the calculated lattice parameter of WC with the different content of Mo_2C. As increasing the Mo_2C contents, the decrease in the WC lattice parameter were observed. It is thought that parameter-composition curve indicate the formation of a series of solid solution.

SEM images of etched surfaces of WC and WC–Mo_2C samples sintered by HFIHS under a pressure of 60 MPa are shown in Fig. 7. SEM images of the microstructure revealed a dense materials with a uniform distribution of the carbide phases and a narrow grain size distribution. In contrast to the spherical shape of the starting or milled powder particles, the grains of the sintered WC are highly faceted with relatively high aspect ratios. No evidence of another phase can be seen, in agreement with the XRD results. The development of well-defined crystallographic facets during sintering of WC reflects

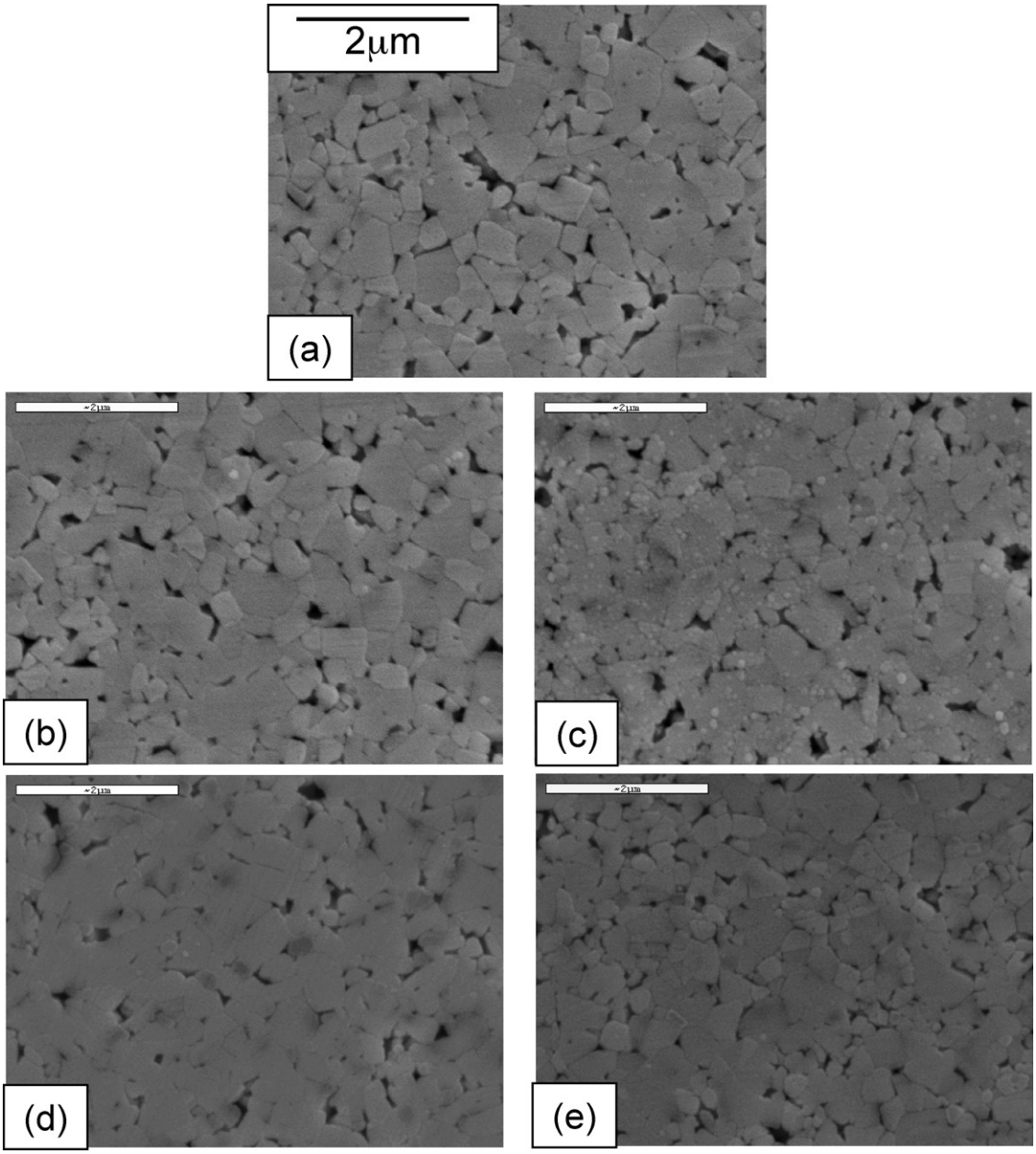

Fig. 7. SEM images of etched surface of WC–*x* wt.%Mo_2C composites sintered by HFIHS (a) WC, (b) WC–1 wt.%Mo_2C, (c) WC–2 wt.%Mo_2C, (d) WC–3 wt.%Mo_2C and (e) WC–6 wt.%Mo_2C.

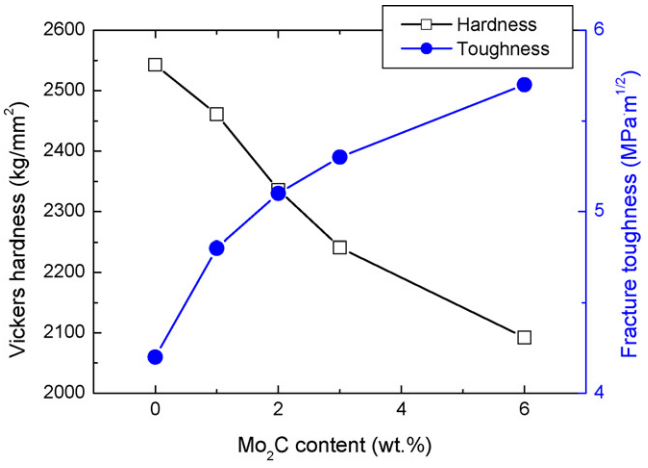

Fig. 8. Vickers hardness and fracture toughness of WC–x wt.%Mo_2C hard materials sintered by HFIHS.

the difference in surface energy of the (0 1 0 0) and (1 0 0 0) planes. Because of this anisotropy, WC grains tend to attain a triangular prism shape, as has been observed before [20]. The average WC grain size of WC–Mo_2C (under 60 MPa, 90% output) determined by the linear intercept method was about 450 nm.

Vickers hardness measurements were made on polished sections of the binderless WC–Mo_2C hard materials using a 10 kg_f load and 15 s dwell time. Indentations with large enough loads produced radial cracks emanating from the corners of the indent. Fracture toughness was calculated from cracks produced in indentations under large loads. The length of these cracks permits an estimation of the fracture toughness of the material by means of Anstis expression [21]

$$K_{IC} = 0.016\left(\frac{E}{H}\right)^{1/2}\frac{P}{C^{3/2}} \quad (1)$$

where E is Young's modulus, H the indentation hardness, P the indentation load, and C is the trace length of the crack measured from the center of the indentation. As in the case of hardness values, the toughness values are derived from the average of 10 measurements. The calculated hardness values and fracture toughness values of binderless WC and WC–Mo_2C composites are shown in Fig. 8 as a function of Mo_2C content for samples produced HFIHS. The Vickers hardness decreased and the fracture toughness increased with increasing Mo_2C content. The calculated hardness and fracture toughness values of WC–1 wt.%Mo_2C with about 450 nm size of WC when made by HFIHS were 2461 kg/mm^2 and 4.8 MPa m$^{1/2}$, respectively, for 60 MPa and an induced current for 90% output of total capacity, 15 kW.

4. Summary

Using high-frequency induction heated sintering (HFIHS), the densification of WC–x wt.%Mo_2C hard materials with grain size of 450 nm were accomplished using ultra fine powders of WC and Mo_2C. A complete densification of the materials was achieved within 1 min. The relative densities of the composite were about 99% for an applied pressure of 60 MPa and an induced current for 90% output of total capacity. The Vickers hardness decreased and the fracture toughness increased with increasing the Mo_2C content. The hardness and fracture toughness values of WC–1 wt.%Mo_2C with about 450 nm size of WC when made by HFIHS were 2461 kg/mm^2 and 4.8 MPa m$^{1/2}$, respectively, for 60 MPa and an induced current for 90% output of total capacity, 15 kW.

Acknowledgement

This work was supported by the grant of Post-Doc. Program, Chonbuk National University, 2006.

References

[1] P. Schwartzkopf, R. Kieffer, Refractory Hard Metals—Boride, Carbide, Nitride and Silicide, MacMillan, New York, 1953.
[2] L.E. Toth, Transition Metal Carbides and Nitrides, Academic Press, New York, 1971.
[3] L. Leclercq, M. Provost, H. Pastor, G. Grimblot, A.M. Hardy, L. Gengembre, J. Catal. 117 (1989) 371–383.
[4] M.J. Ledoux, C.H. Pham, J. Guille, H. Dunlop, J. Catal. 134 (1992) 383–398.
[5] L. Volpe, M. Boudart, J. Solid State Chem. 59 (1985) 348–356.
[6] R. Koc, S.K. Kodambaka, J. Eur. Ceram. Soc. 20 (2000) 1859–1869.
[7] S. Imasato, K. Tokumoto, T. Kitada, S. Kakaguchi, Int. Refract. Met. Hard Mater. 13 (1995) 305–312.
[8] H. Engqvist, N. Axen, S. Hogmark, Tribol. Lett. 4 (1998) 251–258.
[9] M.P. Harmer, R.J. Brook, J. Br. Ceram. Soc. 80 (1981) 147–149.
[10] A. Morell, A. Mermosin, Bull. Am. Ceram. Soc. 59 (1980) 626–629.
[11] M. Omori, Mater. Sci. Eng. A 287 (2000) 183–188.
[12] T.S. Srivatsan, M.R. Woods, M. Petraroli, T.S. Sudarshan, Powder Technol. 122 (2002) 54–60.
[13] H.C. Kim, I.J. Shon, Z.A. Munir, J. Mater. Sci. 40 (2005) 2849–2854.
[14] H.C. Kim, I.J. Shon, J.K. Yoon, S.K. Lee, Z.A. Munir, Int. J. Refract. Met. Hard Mater. 24 (2006) 202–209.
[15] H.C. Kim, I.J. Shon, J.K. Yoon, J.M. Doh, Z.A. Munir, Int. J. Refract. Met. Hard Mater. 24 (2006) 427–431.
[16] H.C. Kim, J.K. Yoon, J.M. Doh, I.Y. Ko, I.J. Shon, Mater. Sci. Eng. A 435–436 (2006) 717–724.
[17] ASTM E112-96, Standard test methods for determining average grain size, 2004.
[18] J.H. Han, D.Y. Kim, Acta Mater. 46 (1998) 2021–2028.
[19] J. Fleischer, T. Masuzawa, J. Schmidt, M. Knoll, J. Mater. Proc. Tech. 149 (2004) 246–249.
[20] A.V. Shatov, S.A. Firstov, I.V. Shatova, Mater. Sci. Eng. A 242 (1998) 7–14.
[21] G.R. Anstis, P. Chantikul, B.R. Lawn, D.B. Marshall, J. Am. Ceram. Soc. 64 (1981) 533–538.